SUPPLEMENTARY MATERIAL

The purpose of this Supplementary Material is to provide intermediate/extended results such that readers with similar but slightly diverging research questions or potential applications can better understand what signals and approaches may work best for their purposes. Sections A and B provide additional results from the feature exploration and feature selection processes, respectively. Section C provides additional figures from Experiment B to help visualize results. Section D provides feature selection results from alternate strategy selection frameworks.

Section A: Feature Exploration, extended

A feature exploration process was outlined in Methods. The intermediate results of this process are provided in this section.

First, a Principal Component Analysis was run for the 35-feature set for Stage 1 and for the 105-feature set for Stage 2. Note that because the authors wanted the variables in the final feature set to be interpretable (i.e., correspond to real-time measurable, physical quantities with which one could draw insight into the biomechanics of stumble recovery), the resulting components were not used as inputs in the model. Instead, this process was performed to provide an estimate of the dimensionality of the feature space [21]. As shown in Fig. A1, approximately 80% of the variance of the set of features can be accounted for with three principal components for Stage 1, and with four principal components for Stage 2. While this does not directly translate to three/four of the features (since principal components are a combination of these features), it does provide an initial benchmark with which to focus the model.

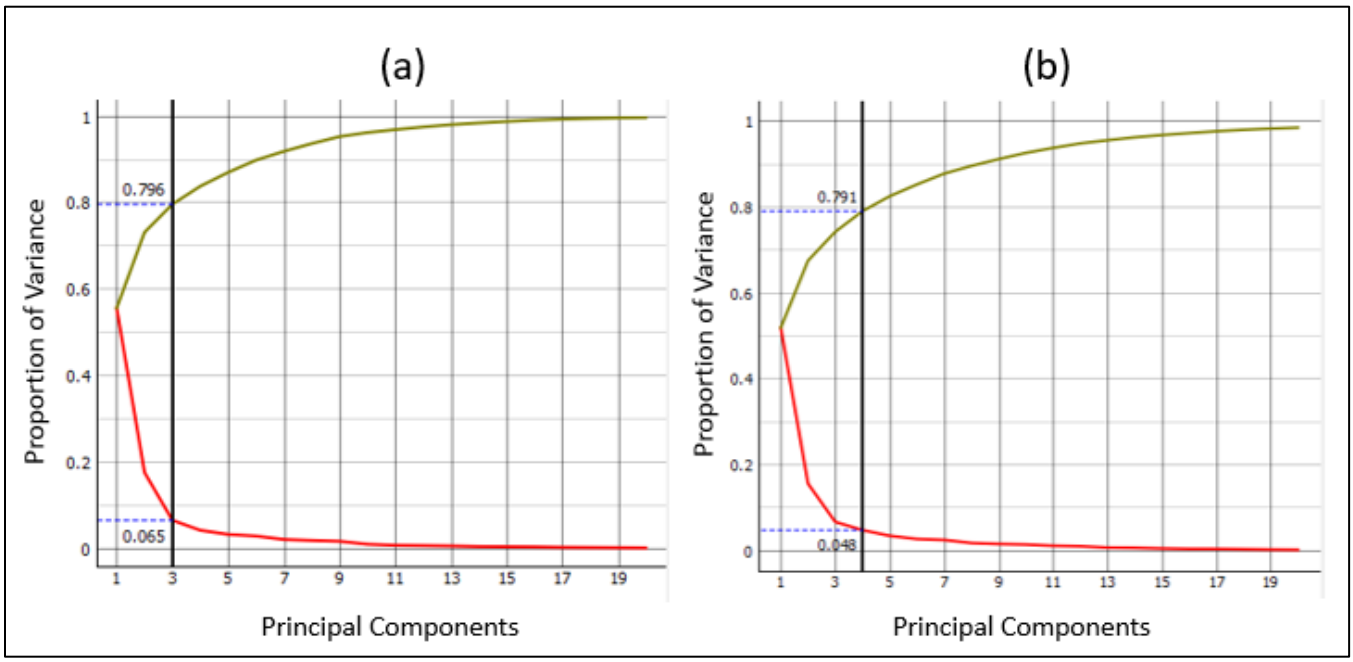

Figure A1. Scree plot from Principal Component Analysis results for 35-feature set for Stage 1 (a) and for 105-feature set for Stage 2 (b). The red line indicates the proportion of variance explained by each principal component independently, and the green line indicates the cumulative proportion of variance explained by the sum of the principal components. Scree plots were generated from the Orange Data Mining Toolbox [24].

Next, the Pearson's Linear Correlation Coefficient was calculated for each feature against every other feature, which gives insight into the redundancy or interdependence of some potential inputs. A visual representation of this is shown in the correlation matrices given in Fig. A2 and A3.

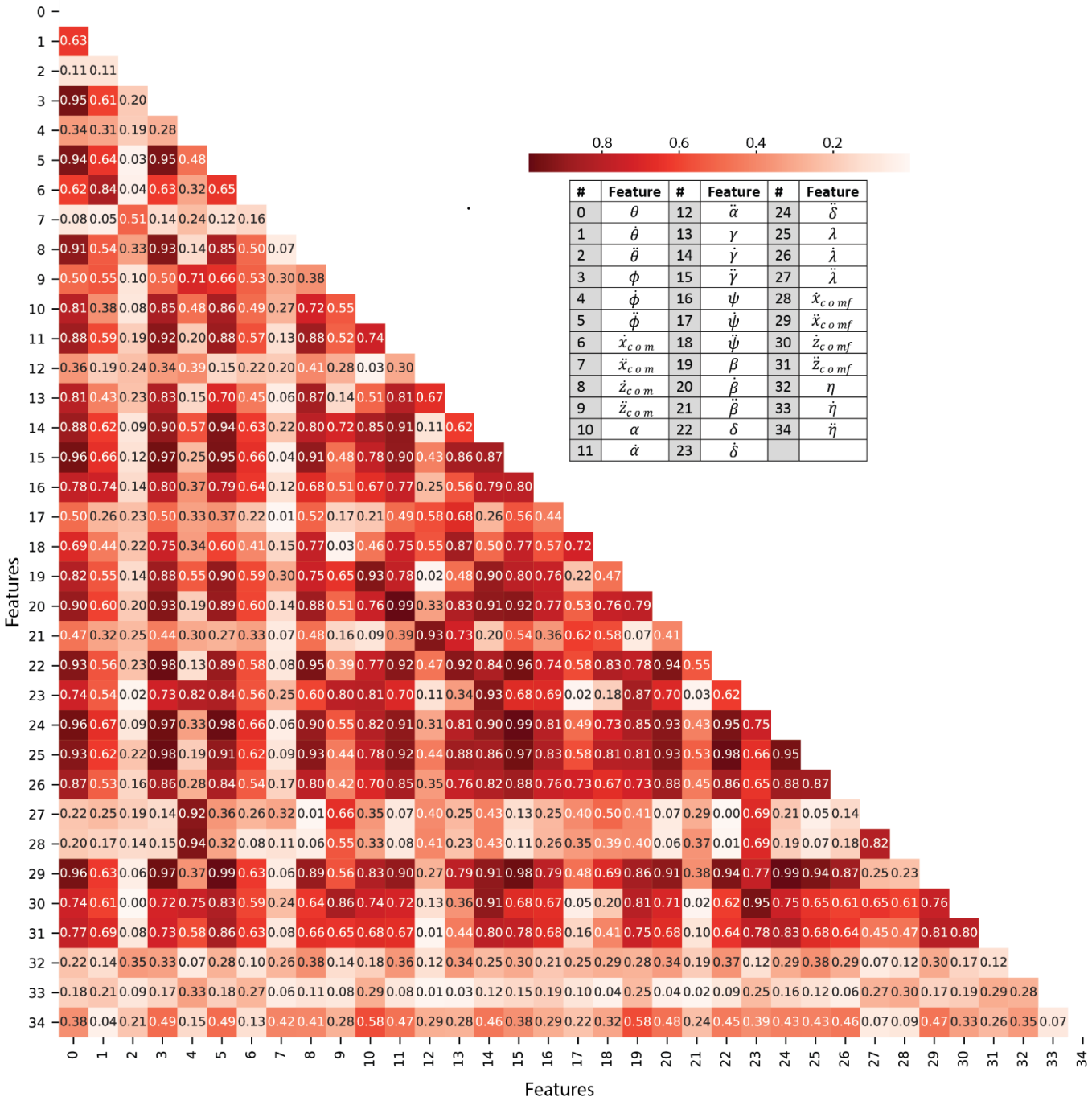

#	Feature	#	Feature	#	Feature
0	θ	12	$\ddot{\alpha}$	24	$\ddot{\delta}$
1	$\dot{\theta}$	13	γ	25	λ
2	$\ddot{\theta}$	14	$\dot{\gamma}$	26	$\dot{\lambda}$
3	ϕ	15	$\ddot{\gamma}$	27	$\ddot{\lambda}$
4	$\dot{\phi}$	16	ψ	28	$\dot{x}_{com f}$
5	$\ddot{\phi}$	17	$\dot{\psi}$	29	$\ddot{x}_{com f}$
6	$\dot{x}_{com}$	18	$\ddot{\psi}$	30	$\dot{z}_{com f}$
7	$\ddot{x}_{com}$	19	β	31	$\ddot{z}_{com f}$
8	$\dot{z}_{com}$	20	$\dot{\beta}$	32	η
9	$\ddot{z}_{com}$	21	$\ddot{\beta}$	33	$\dot{\eta}$
10	α	22	δ	34	$\ddot{\eta}$
11	$\dot{\alpha}$	23	$\dot{\delta}$		

Figure A2. Correlation matrix for the 35 features for Stage 1. Shading corresponds to absolute value of the coefficient, in which darker corresponds to a stronger correlation. Actual correlation values are provided in each square.

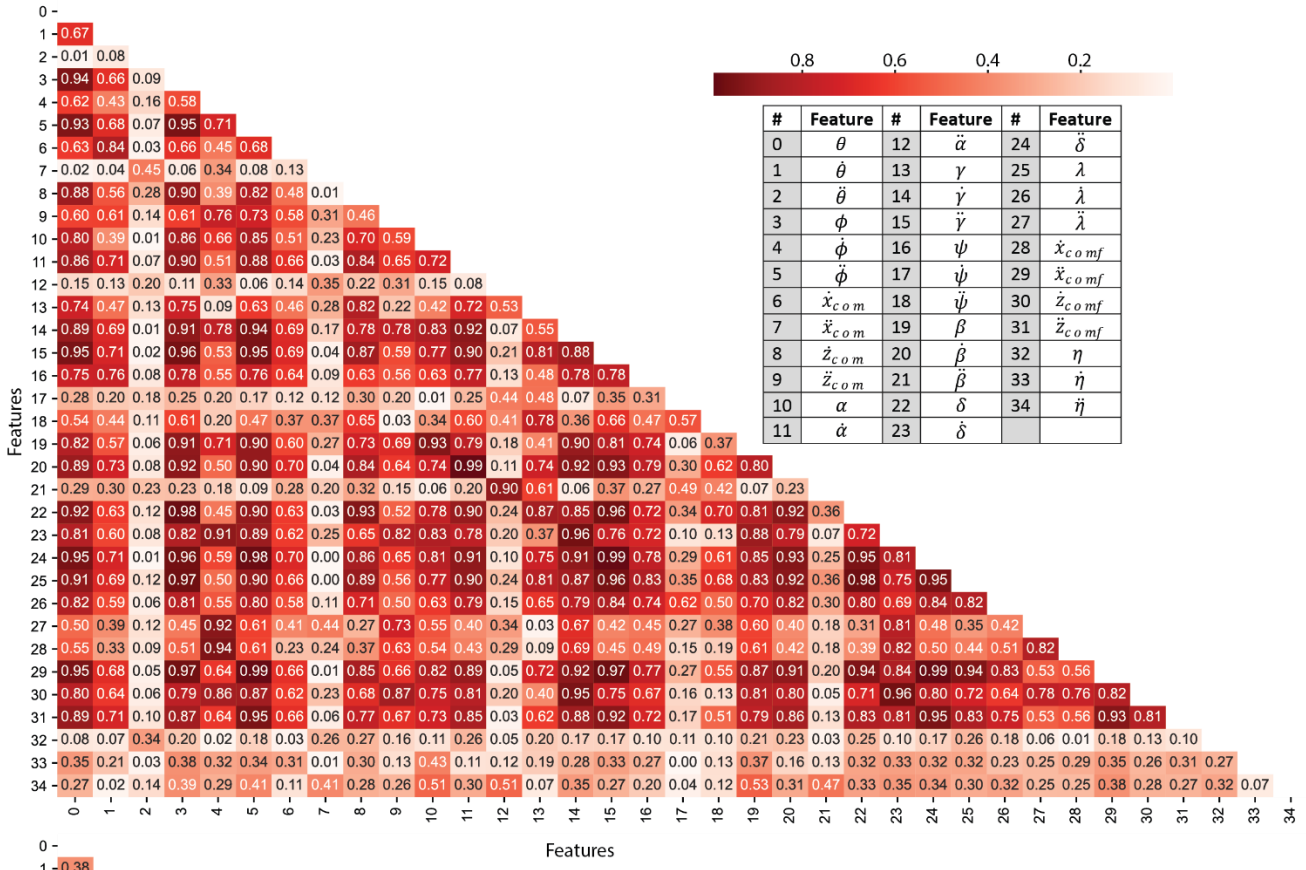

#	Feature	#	Feature	#	Feature
0	θ	12	$\ddot{\alpha}$	24	$\ddot{\delta}$
1	$\dot{\theta}$	13	γ	25	λ
2	$\ddot{\theta}$	14	$\dot{\gamma}$	26	$\dot{\lambda}$
3	ϕ	15	$\ddot{\gamma}$	27	$\ddot{\lambda}$
4	$\dot{\phi}$	16	ψ	28	$\dot{x}_{comf}$
5	$\ddot{\phi}$	17	$\dot{\psi}$	29	$\ddot{x}_{comf}$
6	$\dot{x}_{com}$	18	$\ddot{\psi}$	30	$\dot{z}_{comf}$
7	$\ddot{x}_{com}$	19	β	31	$\ddot{z}_{comf}$
8	$\dot{z}_{com}$	20	$\dot{\beta}$	32	η
9	$\ddot{z}_{com}$	21	$\ddot{\beta}$	33	$\dot{\eta}$
10	α	22	δ	34	$\ddot{\eta}$
11	$\dot{\alpha}$	23	$\dot{\delta}$		

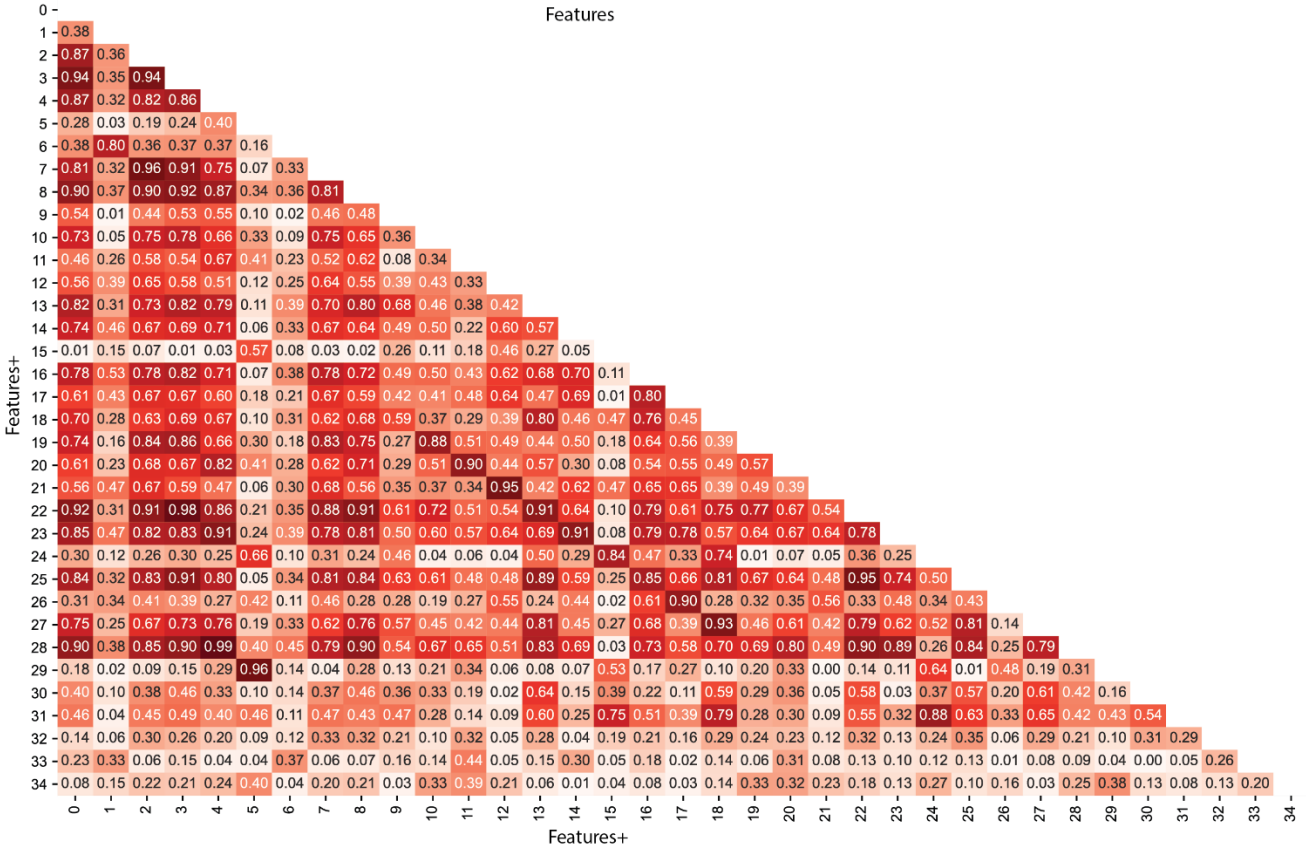

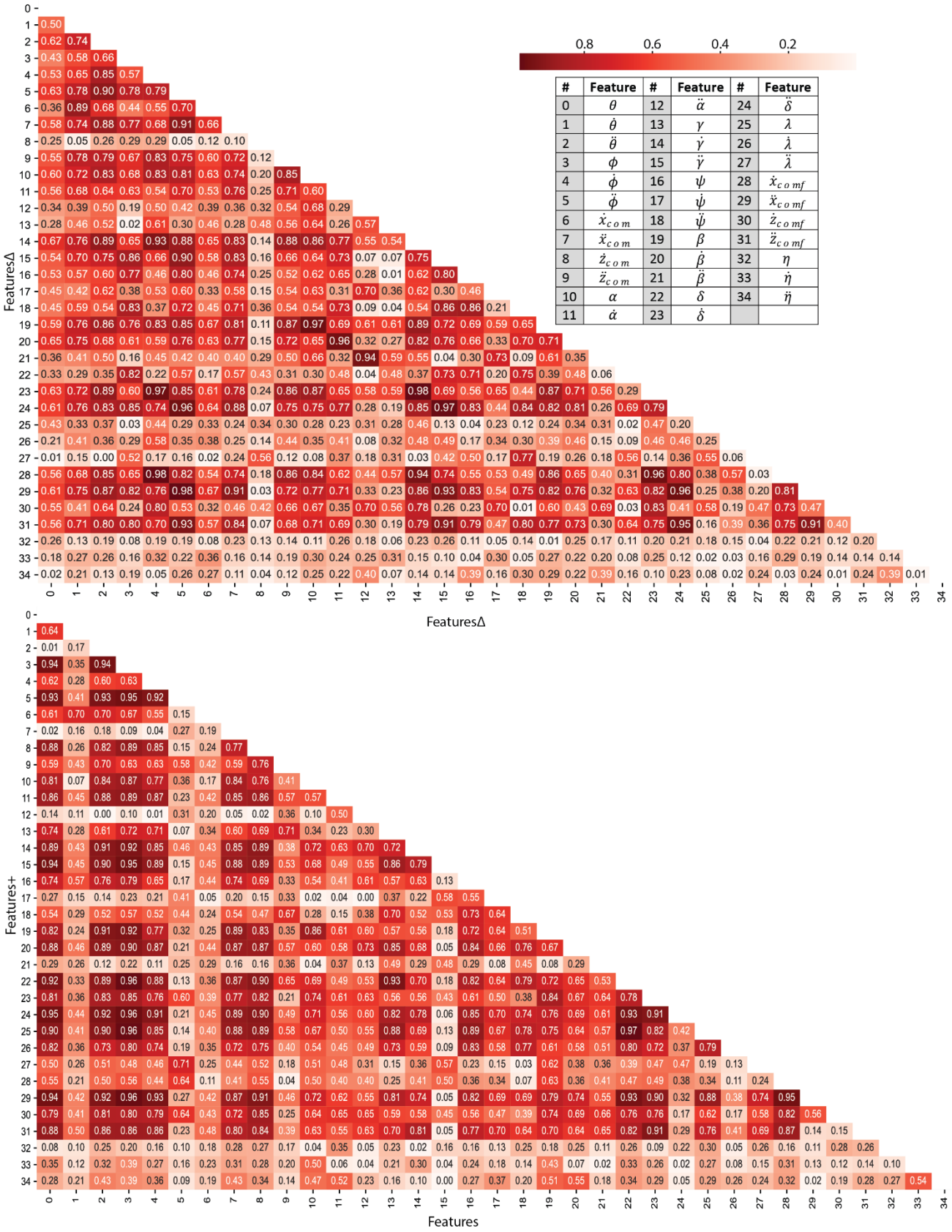

#	Feature	#	Feature	#	Feature
0	θ	12	$\ddot{\alpha}$	24	$\ddot{\delta}$
1	$\dot{\theta}$	13	γ	25	λ
2	$\ddot{\theta}$	14	$\dot{\gamma}$	26	$\dot{\lambda}$
3	ϕ	15	$\ddot{\gamma}$	27	$\ddot{\lambda}$
4	$\dot{\phi}$	16	ψ	28	$\dot{x}_{com f}$
5	$\ddot{\phi}$	17	$\dot{\psi}$	29	$\ddot{x}_{com f}$
6	$\dot{x}_{com}$	18	$\ddot{\psi}$	30	$\dot{z}_{com f}$
7	$\ddot{x}_{com}$	19	β	31	$\ddot{z}_{com f}$
8	$\dot{z}_{com}$	20	$\dot{\beta}$	32	η
9	$\ddot{z}_{com}$	21	$\ddot{\beta}$	33	$\dot{\eta}$
10	α	22	δ	34	$\ddot{\eta}$
11	$\dot{\alpha}$	23	$\dot{\delta}$		

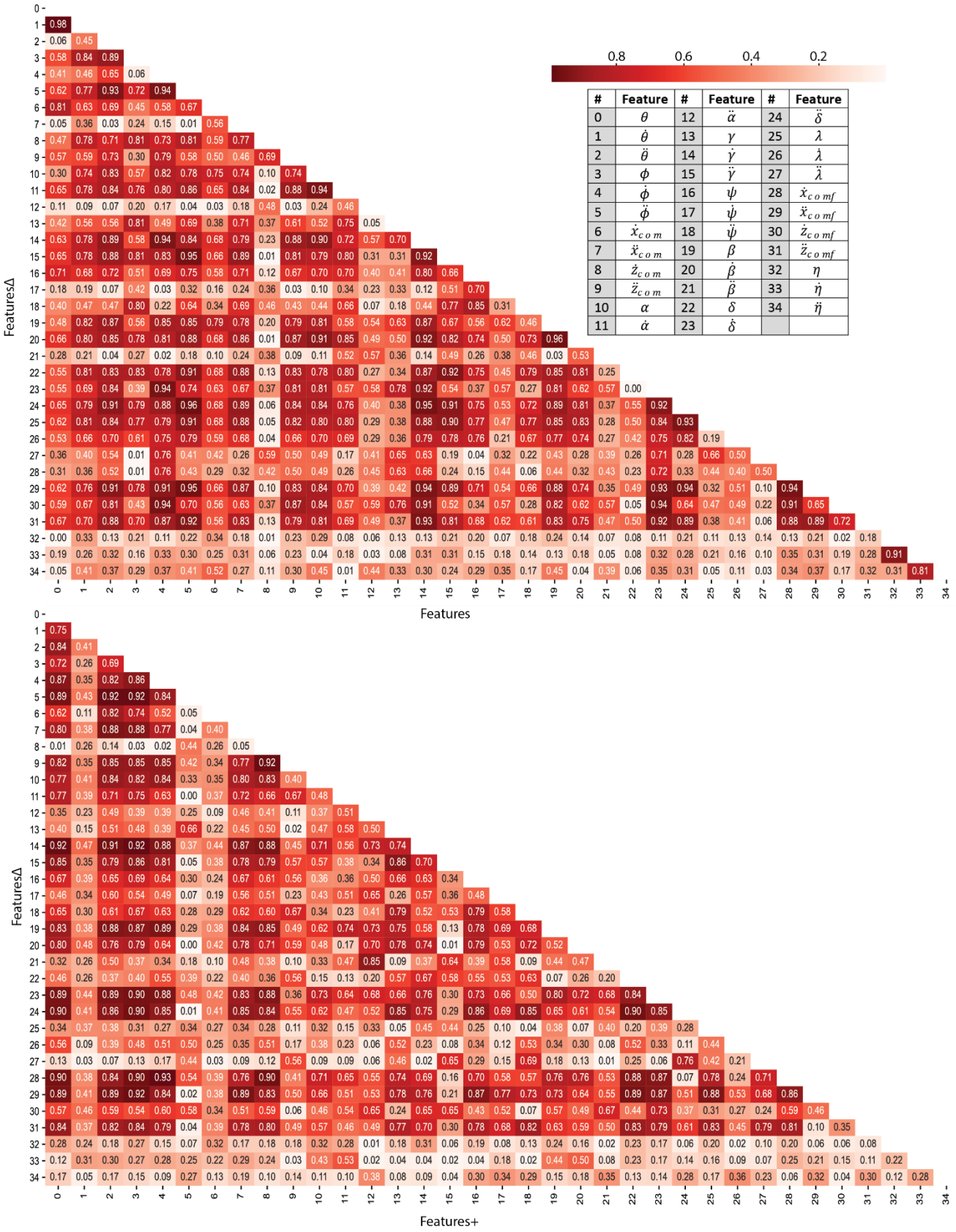

#	Feature	#	Feature	#	Feature
0	θ	12	$\ddot{\alpha}$	24	$\ddot{\delta}$
1	$\dot{\theta}$	13	γ	25	λ
2	$\ddot{\theta}$	14	$\dot{\gamma}$	26	$\dot{\lambda}$
3	ϕ	15	$\ddot{\gamma}$	27	$\ddot{\lambda}$
4	$\dot{\phi}$	16	ψ	28	$\dot{x}_{com f}$
5	$\ddot{\phi}$	17	$\dot{\psi}$	29	$\ddot{x}_{com f}$
6	$\dot{x}_{com}$	18	$\ddot{\psi}$	30	$\dot{z}_{com f}$
7	$\ddot{x}_{com}$	19	β	31	$\ddot{z}_{com f}$
8	$\dot{z}_{com}$	20	$\dot{\beta}$	32	η
9	$\ddot{z}_{com}$	21	$\ddot{\beta}$	33	$\dot{\eta}$
10	α	22	δ	34	$\ddot{\eta}$
11	$\dot{\alpha}$	23	$\dot{\delta}$		

Figure A3. Correlation matrices for the 105 features for Stage 2. The x-axis and y-axis labels indicate whether the features are the measurements taken at perturbation ("Features"), measurements taken 60 ms after the perturbation ("Features+"), or are the difference between the two (FeaturesΔ). Shading corresponds to absolute value of the coefficient, in which darker corresponds to a stronger correlation. Actual correlation values are provided in each square.

Next, each individual feature was considered as its own feature set and fit to a logistic regression model and cross-validated by participant with hyperparameter tuning. The total classification accuracy results for this process are given in Table A1. The purpose of this step was to determine which features independently did well in explaining strategy selection, as well as identify which features individually performed better than swing percentage of perturbation (93.7%).

Table A1. Classification accuracies for individual features as the feature set for Experiment A, Stage 1. Specifically, the second column gives the total classification accuracy from the cross-validation process for Dataset A1 (i.e., the average of the percentage of correctly predicted trials from each participant/fold); the third column gives the average of the balanced accuracies (the average of the true positive rate and true negative rate) from each participant/fold in the cross-validation process for Dataset A1. Features that outperformed swing percentage (93.7%) individually are shaded in gray.

Feature Set	Classification Accuracy	Balanced Accuracy
θ	91.0%	80.2%
$\dot{\theta}$	87.8%	50.0%
$\ddot{\theta}$	87.8%	50.0%
ϕ	94.7%	85.5%
$\dot{\phi}$	87.2%	49.7%
$\ddot{\phi}$	93.1%	76.8%
$\dot{x}_{com}$	88.3%	53.6%
$\ddot{x}_{com}$	87.8%	50.0%
$\dot{z}_{com}$	95.2%	88.6%
$\ddot{z}_{com}$	87.8%	50.0%
α	87.8%	50.0%
$\dot{\alpha}$	96.3%	84.8%
$\ddot{\alpha}$	88.3%	56.4%
γ	95.2%	87.1%
$\dot{\gamma}$	92.1%	65.0%
$\ddot{\gamma}$	90.4%	81.2%
ψ	87.8%	50.0%
$\dot{\psi}$	89.3%	59.5%
$\ddot{\psi}$	94.1%	85.8%
β	87.8%	50.0%
$\dot{\beta}$	95.3%	81.9%
$\ddot{\beta}$	89.9%	69.2%
δ	94.6%	86.8%
$\dot{\delta}$	87.8%	50.0%
$\ddot{\delta}$	91.0%	83.0%
λ	94.6%	86.8%
$\dot{\lambda}$	91.1%	74.7%
$\ddot{\lambda}$	87.8%	53.3%
$\dot{x}_{com,f}$	88.3	57.5%
$\ddot{x}_{com,f}$	93.1%	82.7%
$\dot{z}_{com,f}$	87.8%	50.0%
$\ddot{z}_{com,f}$	87.8%	50.0%

η	88.3%	53.5%
$\dot{\eta}$	87.8%	50.0%
$\ddot{\eta}$	88.3%	51.7%

This process was repeated for Stage 2 and results are tabulated in Table A2.

Table A2. Classification accuracies for individual features as the feature set for Experiment A, Stage 2. Specifically, the second column gives the total classification accuracy from the cross-validation process for Dataset A2 (i.e., the average of the percentage of correctly predicted trials from each participant/fold); the third column gives the average of the balanced accuracies (the average of the true positive rate and true negative rate) from each participant/fold in the cross-validation process for Dataset A2. Note that no subscript with the feature variable indicates that the feature is the measurement taken at the instant of perturbation, the subscript "+" indicates that feature is the measurement taken 60 ms after the perturbation, and the subscript "Δ" indicates that the feature is the difference between the two aforementioned measurements, as explained in Methods. Features that outperformed swing percentage (85.6%) individually are shaded in gray.

Feature Set	Classification Accuracy	Balanced Accuracy
θ	82.7%	79.9%
$\dot{\theta}$	72.4%	60.2%
$\ddot{\theta}$	75.8%	50.0%
ϕ	88.3%	85.1%
$\dot{\phi}$	75.8%	50.0%
$\ddot{\phi}$	86.7%	85.7%
$\dot{x}_{com}$	70.6%	55.3%
$\ddot{x}_{com}$	75.8%	50.0%
$\dot{z}_{com}$	83.6%	82.6%
$\ddot{z}_{com}$	74.1%	49.1%
α	80.8%	67.5%
$\dot{\alpha}$	84.2%	78.3%
$\ddot{\alpha}$	75.8%	50.0%
γ	81.1%	77.3%
$\dot{\gamma}$	84.7%	70.6%
$\ddot{\gamma}$	80.4%	76.4%
ψ	75.4%	64.4%
$\dot{\psi}$	74.5%	62.7%
$\ddot{\psi}$	82.6%	77.0%
β	83.3%	66.3%
$\dot{\beta}$	85.9%	82.2%
$\ddot{\beta}$	76.4%	57.1%
δ	85.5%	84.1%
$\dot{\delta}$	76.1%	52.5%
$\ddot{\delta}$	84.5%	82.4%
λ	81.9%	78.8%
$\dot{\lambda}$	81.2%	73.8%
$\ddot{\lambda}$	75.8%	50.0%
$\dot{x}_{com,f}$	75.8%	50.0%
$\ddot{x}_{com,f}$	86.5%	84.6%
$\dot{z}_{com,f}$	75.2%	49.7%
$\ddot{z}_{com,f}$	78.0%	63.6%
η	74.6%	49.3%
$\dot{\eta}$	74.5%	49.0%

$\ddot{\eta}$	80.7%	57.7%
θ_+	82.2%	77.9%
$\dot{\theta}_+$	75.8%	50.0%
$\ddot{\theta}_+$	86.3%	83.4%
ϕ_+	86.9%	82.8%
$\dot{\phi}_+$	86.1%	83.7%
$\ddot{\phi}_+$	75.2%	49.6%
$\dot{x}_{com+}$	72.4%	48.2%
$\ddot{x}_{com+}$	83.9%	80.2%
$\dot{z}_{com+}$	81.7%	79.0%
$\ddot{z}_{com+}$	81.1%	71.8%
α_+	78.6%	58.7%
$\dot{\alpha}_+$	78.7%	57.7%
$\ddot{\alpha}_+$	75.5%	54.4%
γ_+	80.7%	77.6%
$\dot{\gamma}_+$	77.4%	60.9%
$\ddot{\gamma}_+$	74.5%	49.1%
ψ_+	80.5%	77.6%
$\dot{\psi}_+$	79.2%	63.8%
$\ddot{\psi}_+$	82.4%	76.7%
β_+	80.7%	62.2%
$\dot{\beta}_+$	83.5%	68.2%
$\ddot{\beta}_+$	77.0%	57.2%
δ_+	85.0%	82.8%
$\dot{\delta}_+$	81.9%	72.3%
$\ddot{\delta}_+$	75.8%	63.5%
λ_+	87.2%	84.2%
$\dot{\lambda}_+$	74.0%	54.1%
$\ddot{\lambda}_+$	86.2%	82.8%
$\dot{x}_{com,f+}$	87.3%	86.0%
$\ddot{x}_{com,f+}$	73.9%	48.8%
$\dot{z}_{com,f+}$	77.7%	65.7%
$\ddot{z}_{com,f+}$	78.6%	71.1%
η_+	74.6%	49.3%
$\dot{\eta}_+$	75.8%	50.0%
$\ddot{\eta}_+$	75.8%	50.0%
θ_Δ	73.5%	54.0%
$\dot{\theta}_\Delta$	77.7%	67.1%
$\ddot{\theta}_\Delta$	82.1%	75.9%
ϕ_Δ	87.2%	83.8%
$\dot{\phi}_\Delta$	81.8%	69.3%
$\ddot{\phi}_\Delta$	87.6%	86.8%
$\dot{x}_{com\Delta}$	77.5%	67.8%
$\ddot{x}_{com\Delta}$	82.0%	80.5%
$\dot{z}_{com\Delta}$	73.9%	48.8%
$\ddot{z}_{com\Delta}$	79.8%	65.7%
α_Δ	81.9%	69.2%
$\dot{\alpha}_\Delta$	85.1%	82.0%
$\ddot{\alpha}_\Delta$	75.8%	50.0%
γ_Δ	75.2%	49.7%

$\dot{\gamma}_{\Delta}$	83.0%	73.1%
$\ddot{\gamma}_{\Delta}$	81.1%	75.1%
ψ_{Δ}	83.6%	80.4%
$\dot{\psi}_{\Delta}$	75.8%	55.2%
$\ddot{\psi}_{\Delta}$	85.0%	80.2%
β_{Δ}	84.7%	71.0%
$\dot{\beta}_{\Delta}$	79.4%	75.9%
$\ddot{\beta}_{\Delta}$	75.8%	51.0%
δ_{Δ}	77.4%	68.2%
$\dot{\delta}_{\Delta}$	81.1%	66.9%
$\ddot{\delta}_{\Delta}$	83.1%	79.5%
λ_{Δ}	75.8%	50.0%
$\dot{\lambda}_{\Delta}$	77.5%	62.6%
$\ddot{\lambda}_{\Delta}$	72.8%	56.2%
$\dot{x}_{com,f\Delta}$	82.2%	70.6%
$\ddot{x}_{com,f\Delta}$	86.4%	85.0%
$\dot{z}_{com,f\Delta}$	75.8%	50.0%
$\ddot{z}_{com,f\Delta}$	82.9%	73.4%
η_{Δ}	75.8%	50.0%
$\dot{\eta}_{\Delta}$	75.8%	50.5%
$\ddot{\eta}_{\Delta}$	74.0%	48.8%

Section B: Feature Selection, extended

As mentioned in the main text, the top subsets for each stage (i.e., the subsets with the highest classification accuracies after cross validation and hyperparameter tuning, obtained via a wrapper method on Dataset A) were recorded for each stage (and tested on Dataset B to choose final feature set). These top subsets are listed in Tables B1 and B2 for Stage 1 and Stage 2, respectively, with the final feature set reported in the main text shaded in gray.

Table B1. Top four subsets for Stage 1. The first column lists the features in the subset, the second column reports the total classification accuracy from cross-validation by participant with hyperparameter tuning on Experiment A, and the third columns reports the classification accuracy when trained on Dataset A (without Participant 3's trials) and tested on Dataset B with hyperparameter tuning. The final subset for Stage 1, reported in main text, is shaded in gray.

Feature set	Classification Accuracy for Dataset A	Classification Accuracy for testing on Dataset B
$\ddot{\phi}, \dot{z}_{com}, \dot{\gamma}, \ddot{\lambda}$	99.5%	96.2%
$\theta, \dot{z}_{com}, \dot{\gamma}, \ddot{\lambda}$	99.0%	100.0%
$\dot{z}_{com}, \dot{\gamma}, \ddot{\psi}, \ddot{\eta}$	99.0%	88.5%
$\dot{z}_{com}, \dot{\gamma}, \ddot{\lambda}, \ddot{z}_{com,f}$	99.0%	96.2%

Table B2. Top 28 subsets for Stage 2. The first column lists the features in the subset, the second column reports the total classification accuracy from cross-validation by participant with hyperparameter tuning on Experiment A, and the third columns reports the classification accuracy when trained on Dataset A (without Participant 3's trials) and tested on Dataset B with hyperparameter tuning. The final subset for Stage 2, reported in main text, is shaded in gray.

Feature set	Classification Accuracy for Dataset A	Classification Accuracy for testing on Dataset B
$\dot{x}_{com,f}, \ddot{\phi}_{\Delta}, \dot{z}_{com\Delta}, \ddot{\delta}_{\Delta}$	96.1%	87.0%
$\ddot{\phi}, \ddot{\gamma}, \ddot{x}_{com,f}, \dot{z}_{com\Delta}$	95.2%	82.6%

$\ddot{x}_{com,f+}\ \ddot{\phi}_{\Delta}\ ,\dot{z}_{com\Delta}\ ,\ddot{\delta}_{\Delta}$	95.1%	87.0%
$\dot{\phi}\ \ddot{\phi}_{\Delta}\ ,\dot{z}_{com\Delta}\ ,\ddot{\delta}_{\Delta}$	95.0%	87.0%
$\ddot{z}_{com},\ddot{x}_{com,f+}\ \dot{z}_{com\Delta}\ ,\ddot{\delta}_{\Delta}$	94.9%	82.6%
$\ddot{z}_{com},\ddot{x}_{com,f+}\ \ddot{\phi}_{\Delta}\ ,\ddot{\delta}_{\Delta}$	94.9%	87.0%
$\theta,\ddot{\psi},\ddot{x}_{com,f}\ \dot{z}_{com\Delta}$	94.6%	91.3%
$\ddot{z}_{com}\ ,\ddot{x}_{com,f}\ ,\ddot{\theta}_{+},\ddot{\delta}_{\Delta}$	94.6%	91.3%
$\ddot{z}_{com},\ddot{x}_{com,f}\ ,\dot{x}_{com\Delta}\ ,\ddot{\gamma}_{\Delta}$	94.6%	87.0%
$\ddot{z}_{com},\ddot{x}_{com,f}\ ,\ddot{\theta}_{+},\ddot{\delta}_{\Delta}$	94.6%	91.3%
$\ddot{z}_{com},\ddot{x}_{com,f}\ ,\dot{x}_{com\Delta}\ ,\ddot{\gamma}_{\Delta}$	94.6%	87.0%
$\ddot{z}_{com},\ddot{\phi}_{\Delta},\ \ddot{\delta}_{\Delta},\dot{x}_{com,f\Delta}$	94.5%	82.6%
$\alpha\ ,\ddot{\psi}\ ,\ddot{x}_{com,f},\dot{z}_{com\Delta}$	94.5%	87.0%
$\ddot{z}_{com},\ddot{\phi}_{\Delta},\ \ddot{\delta}_{\Delta}\ ,\dot{x}_{com,f\Delta}$	94.5%	82.6%
$\alpha,\ddot{\psi}\ ,\ddot{x}_{com,f},\dot{z}_{com\Delta}$	94.5%	87.0%
$\ddot{x}_{com,f}\ ,\dot{z}_{com\Delta}\ ,\dot{\psi}_{\Delta},\ddot{\gamma}_{\Delta}$	94.5%	82.6%
$\ddot{x}_{com,f}\ ,\ddot{\phi}_{\Delta}\ ,\dot{z}_{com\Delta}\ ,\ddot{\delta}_{\Delta}$	94.5%	87.0%
$\ddot{\phi}_{+}\ ,\ddot{\phi}_{\Delta}\ ,\dot{z}_{com\Delta}\ ,\ddot{\delta}_{\Delta}$	94.5%	87.0%
$\ddot{\phi},\ddot{z}_{com}\ ,\ddot{\delta}\ ,\gamma_{+}$	94.4%	91.3%
$\ddot{z}_{com}\ ,\ddot{\delta}_{+}\ ,\ddot{\phi}_{\Delta}\ ,\ddot{\gamma}_{\Delta}$	94.4%	87.0%
$\ddot{\delta},\ddot{x}_{com,f+},\ddot{\phi}_{\Delta},\ \dot{z}_{com\Delta}$	94.4%	87.0%
$\dot{\phi}_{\Delta}\ ,\ddot{\phi}_{\Delta}\ ,\dot{z}_{com\Delta}\ ,\ddot{\delta}_{\Delta}$	94.3%	82.6%
$\ddot{z}_{com}\ ,\dot{\delta}\ ,\dot{\phi}_{\Delta},\ \ddot{\delta}_{\Delta}$	94.3%	87.0%
$\ddot{\theta},\ddot{\psi},\ddot{x}_{com,f},\dot{z}_{com\Delta}$	94.0%	87.0%
$\ddot{\phi}\ ,\ddot{z}_{com}\ ,\dot{z}_{com+},\ddot{\gamma}_{\Delta}$	94.0%	82.6%
$\ddot{\phi}\ \ ,\ddot{\delta}\ ,\gamma_{+},\dot{z}_{com\Delta}$	94.0%	95.7%
$\ddot{z}_{com}\ ,\ddot{x}_{com,f}\ ,\ddot{\theta}_{+}\ ,\ddot{\gamma}_{\Delta}$	94.0%	91.3%
$\ddot{\psi},\ddot{x}_{com,f},\dot{z}_{com\Delta}$	94.0%	82.6%

As mentioned in the main text, the authors performed feature selection without any limit on feature type or number (up to four). The following table tabulates top performing subsets given described constraints, which may be important depending on the readers' application/research question.

Table B3: Top feature subsets given constraints on feature type and number of features for Stage 1. The first column indicates the maximum number of features that were allowed in the subset, the second column indicates what type of feature is allowed in the subset, the third column reports which features are in the subset, with the corresponding classification accuracy (from cross validation by participant with hyperparameter tuning with Experiment A) recorded in the fourth column.

Constraint 1: Max Number of Features	Constraint 2: Feature Type	Best Feature set	Classification Accuracy
2	All	$\dot{\alpha},\phi$	97.9%
		$\dot{\alpha},\gamma$	97.9%
		$\dot{\alpha},\ddot{\beta}$	97.9%
		$\dot{\alpha},\ddot{\lambda}$	97.9%
		$\dot{z}_{com},\dot{\beta}$	97.9%
4	Only Whole Body (features from Fig. 2a)	$\ddot{\theta},\phi,\dot{z}_{com},\ddot{\eta}$	97.9%
		$\phi,\dot{\phi},z_{com},\ddot{\eta}$	97.9%
		$\phi,\ddot{x}_{com},\dot{z}_{com},\ddot{\eta}$	97.9%
		$\phi,\dot{z}_{com},\ddot{z}_{com},\ddot{\eta}$	97.9%
		$\phi,\dot{z}_{com},\eta,\ddot{\eta}$	97.9%

4	Only External Angles and Derivatives (Fig. 2b)	$\dot{\beta}, \ddot{\beta}$ $\dot{\beta}, \delta$ $\dot{\beta}, \lambda$	97.4% 97.4% 97.4%
4	Only Internal Angles and Derivatives (Fig. 2c)	$\dot{\alpha}, \gamma$	97.9%
2	Only Position	γ, δ	95.8%
4	Only Position	$\theta, \gamma, \delta, \eta$	96.3%
2	Only Velocity	$\dot{z}_{com}, \dot{\beta}$	97.9%
4	Only Velocity	$\dot{\phi}, \dot{z}_{com}, \dot{\alpha}, \dot{z}_{com,f}$	98.5%
2	Only Acceleration	$\ddot{\theta}, \ddot{\phi}$	96.3%
4	Only Acceleration	$\ddot{\theta}, \ddot{z}_{com}, \ddot{\alpha}, \ddot{x}_{com,f}$ $\ddot{\theta}, \ddot{z}_{com}, \ddot{\beta}, \ddot{x}_{com,f}$ $\ddot{\phi}, \ddot{z}_{com}, \ddot{\gamma}, \ddot{x}_{com,f}$	97.9% 97.9% 97.9%

It is notable that a very high classification accuracy can still be obtained with just two inputs for Stage 1. Additionally, subsets with features measurable from the ipsilateral limb alone (analogous to signals measurable by sensors on a potential intervention such as a prosthesis) also reach substantially high classification accuracy. This information may be useful for prosthesis designers looking to monitor and correct for stumble perturbations.

Table B4: Top feature subsets given constraints on feature type and number of features for Stage 2. The first column indicates the maximum number of features that were allowed in the subset, the second column indicates what type of feature is allowed in the subset (in which "at perturbation" corresponds to the value at perturbation, "+" corresponds to the value 60 ms after perturbation, and "Δ" corresponds to the difference between the two), the third column reports which features are in the subset, with the corresponding classification accuracy (from cross validation by participant with hyperparameter tuning with Experiment A) recorded in the fourth column.

Constraint 1: Max Number of Features	Constraint 2: Feature Type	Best Feature set	Classification Accuracy
2	All	$\dot{\beta}, \ddot{\phi}_{\Delta}$	91.1%
3	All	$\ddot{\gamma}, \ddot{x}_{com,f}, \dot{z}_{com\Delta}$	94.0%
2	Only features at perturbation	$\ddot{\theta}, \dot{z}_{com}$	90.0%
3	Only features at perturbation	$\ddot{\phi}, \ddot{z}_{com}, \ddot{\delta}$	92.5%
4	Only features at perturbation	$\ddot{\phi}, \dot{z}_{com}, \ddot{\alpha}, \ddot{\gamma}$	93.4%
2	Only features+	β_+, λ_+	89.8%
3	Only features+	$\ddot{\theta}_+, \beta_+, \ddot{\lambda}_+$	91.1%
4	Only features+	$\ddot{\theta}_+, \ddot{z}_{com+}, \dot{\psi}_+, \lambda_+$	91.7%
2	Only features **Δ**	$\dot{\theta}_{\Delta}, \phi_{\Delta}$	89.9%
3	Only features **Δ**	$\ddot{\phi}_{\Delta}, \dot{z}_{com\Delta}, \delta_{\Delta}$	91.8%
4	Only features **Δ**	$\dot{\phi}_{\Delta}, \ddot{\phi}_{\Delta}, \dot{z}_{com\Delta}, \ddot{\delta}_{\Delta}$	94.4%
2	Only Whole Body (features from Fig. 2a)	$\ddot{\eta}, \theta_+$	90.9%
3	Only Whole Body (Fig. 2a)	$\dot{\theta}, \ddot{\eta}, \ddot{z}_{com+}$	90.6%
4	Only Whole Body (Fig. 2a)	$\ddot{z}_{com}, \ddot{\eta}, \ddot{\theta}_+, \dot{\phi}_{\Delta}$	92.2%
2	Only External Angles (Fig. 2b)	β, λ_+	89.9%
3	Only External Angles (Fig. 2b)	$\beta, \lambda_+, \lambda_{\Delta}$	91.7%
2	Only Internal Angles (Fig 2.c)	α, ψ_{Δ}	89.4%
3	Only Internal Angles (Fig. 2c)	$\alpha, \dot{\alpha}, \ddot{\psi}_{\Delta}$	90.0%
4	Only Internal Angles (Fig. 2c)	$\dot{\gamma}, \psi, \dot{\psi}, \ddot{\psi}$	90.6%
2	Only Position	β, ψ_{Δ}	89.9%
3	Only Position	$\beta, \beta_+, \psi_{\Delta}$	90.6%

4	Only Position	$\alpha, \beta, \psi_\Delta, \eta_\Delta$	91.7%
2	Only Velocity	$\dot{z}_{com}, \dot{\psi}_+$	89.3%
3	Only Velocity	$\dot{\phi}_+, \dot{\psi}_+, \dot{z}_{com\Delta}$	92.2%
2	Only Acceleration	$\ddot{\phi}_\Delta, \ddot{\alpha}_\Delta$	89.8%
3	Only Acceleration	$\ddot{\delta}_+, \ddot{z}_{com,f+}, \ddot{\psi}_\Delta$	91.7%
4	Only Acceleration	$\ddot{\gamma}, \ddot{\phi}_\Delta, \ddot{\delta}_\Delta, \ddot{\eta}_\Delta$	92.8%

Section C: Experiment B Results, extended

In the main text the authors suggest that the model extends across walking speeds based on prediction results from a single participant walking at two additional speeds. The following figures and tables break down Experiment B results in more detail (as was done in the main text for Experiment A).

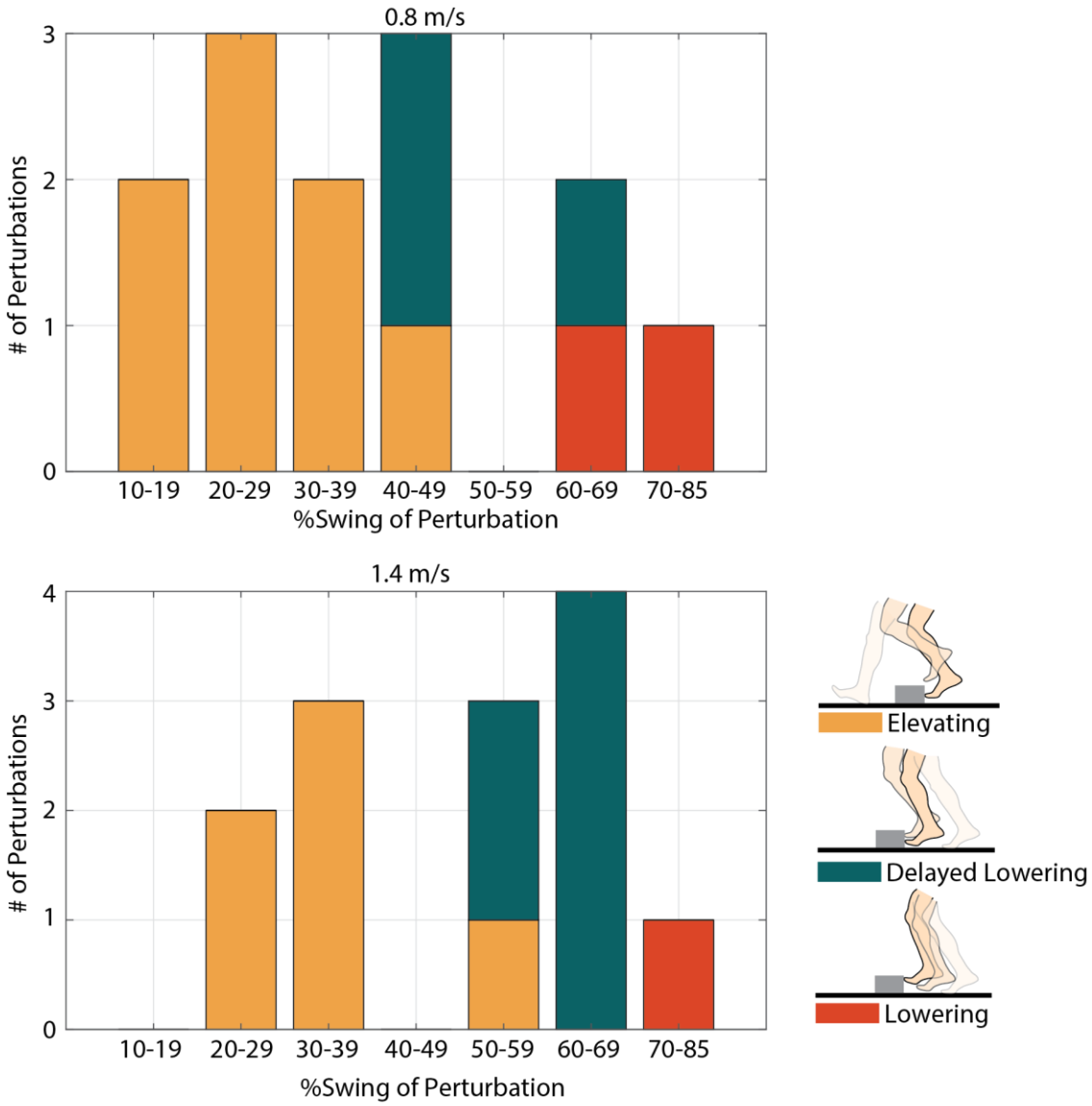

Figure C1. Breakdown of strategy used for each binned percentage of swing phase for each walking speed for Experiment B.

(a)

	Predicted Initially Elevating	Predicted Lowering	Total
Actual Initially Elevating	23	0	23
Actual Lowering	0	3	3
Total	23	3	26

(b)

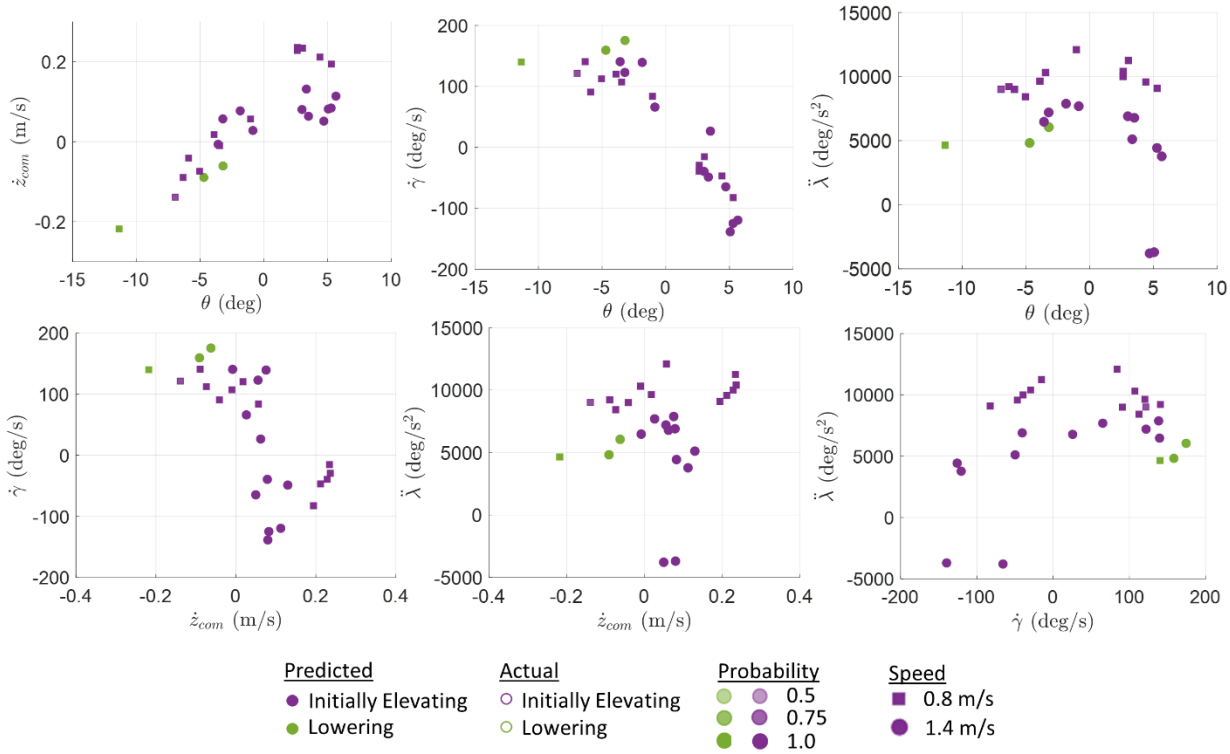

Figure C2. (a) The confusion matrix of prediction results and (b) scatter plots of the datasets as a function of features used for Stage 1 of the strategy selection process for Dataset B. For Stage 1, the scatter plot depicts contralateral foot to center-of-mass (CF-to-COM) angle (θ), knee angular velocity ($\dot{\gamma}$), body COM vertical velocity ($\dot{z}_{com}$), and foot angular acceleration ($\ddot{\lambda}$) at the time of perturbation for each of the 188 trials. Refer to Fig. 2 for diagrams of these physical quantities. Purple indicates Initially Elevating, while green indicates Lowering. Marker outline color represents the actual strategy used, while marker fill color represents the model's prediction. Shading of the marker fill indicates the probability of being that strategy as indicated by the logistic regression model, in which transparent indicates a probability of 0.5 and opaque indicates a probability of 1.0. The marker shapes of square and circle indicate walking speeds of 0.8 m/s and 1.4 m/s, respectively.

(a)

	Predicted Elevating	Predicted Delayed Lowering	Total
Actual Elevating	13	1	14
Actual Delayed Lowering	0	9	9
Total	13	10	23

(b)

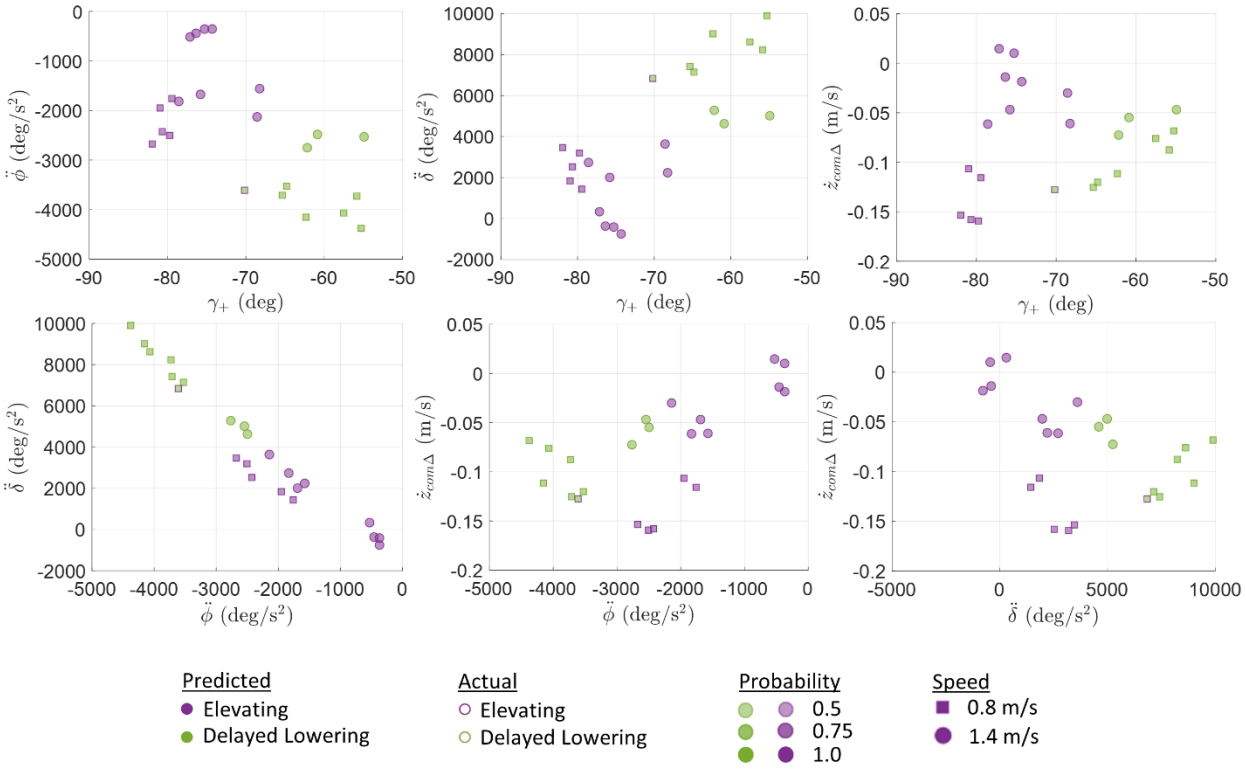

Figure C3. (a) The confusion matrix of prediction results and (c) scatter plots of the datasets as a function of features used for Stage 2 of the strategy selection process for Dataset B. For Stage 2, the scatter plot depicts the IF-to-COM angular acceleration ($\ddot{\phi}$) and shank angular acceleration ($\ddot{\delta}$) at the time of perturbation, knee angle 60 ms after the perturbation (γ_+), and change in body COM vertical velocity ($\dot{z}_{com\Delta}$) for each of the 165 trials. Note that the "+" indicates that the feature is the measurement taken 60 ms after perturbation, and that the "Δ" indicates that the feature is the change in value from the instant of perturbation to 60 ms after the perturbation. Refer to Fig. 2 for diagrams depicting each physical quantity. Purple indicates Elevating while green indicates Delayed Lowering. Marker outline color represents the actual strategy used, while marker fill color represents the model's prediction. Shading of the marker fill indicates the probability of being that strategy as indicated by the logistic regression model, in which transparent indicates a probability of 0.5 and opaque indicates a probability of 1.0. The marker shapes of square and circle indicate walking speeds of 0.8 m/s and 1.4 m/s, respectively.

Section D: Consideration of other strategy selection frameworks

Note that the model that the authors believed best described the strategy selection process was presented, validated, and discussed in this paper; however, in the model development process, many strategy selection frameworks were considered. As explained in Methods, the proposed 2-stage strategy selection process seems most physiologically relevant based on prior literature's EMG results [1] in conjunction with the timing of the foot trajectory after perturbation. To be exhaustive, though, the wrapper method with cross validation by participant and hyperparameter tuning for Experiment A was run with two additional frameworks, with classification accuracy results reported in Table D1. The first involves an instantaneous decision, in which at perturbation the body simply chooses one of the three strategies (i.e., Elevating, Delayed Lowering, or Lowering). The second combines the Delayed Lowering and Lowering strategies into one class, in which at perturbation the body chooses between Elevating and Lowering (i.e., Delayed Lowering and Lowering). Table D1 shows enumerates the top performing feature sets (out of the same 35 features from Fig. 2) for each framework along with their corresponding classification accuracy. Note that the classification accuracies are lower than the RTMM. Table D1 also shows classification accuracy for swing percentage as the feature set; swing percentage still does not outperform the real-time measurable, physical quantities as features, even for these inferior strategy selection frameworks.

Table D1. Classification accuracy results for additional strategy selection frameworks. Specifically, the third column gives the total classification accuracy from the cross-validation process for Experiment A (i.e., the average of the percentage of correctly predicted trials from each participant/fold).

Framework	**Max number of Features: Feature Set**	**Classification Accuracy**
Choose 1 of 3 strategies at instant of perturbation	2: ϕ, γ	86.8%
	3: θ, $\dot{\alpha}$, $\ddot{\beta}$	88.8%
	4: $\dot{z}_{com}$, γ, $\ddot{\beta}$, $\ddot{x}_{com,f}$	91.5%
	Swing Percentage	80.3%
Group Lowering and Delayed Lowering as one strategy; choose between elevating and lowering at instant of perturbation	2: ϕ, β	91.1%
	3: $\ddot{\phi}$, $\dot{z}_{com}$, $\ddot{\delta}$	93.2%
	4: $\ddot{\phi}$, $\dot{z}_{com}$, $\ddot{\alpha}$, $\ddot{\gamma}$	93.7%
	Swing Percentage	87.6%